Pergamon

Int. J. Heat Mass Transfer. Vol. 37, No. 5, pp. 803–818, 1994

0017–9310/94 $6.00+0.00

Quenching experiments with a circular test section of medium thermal capacity under forced convection of water

X. C. HUANG, G. BARTSCH and D. SCHROEDER-RICHTER
Institut für Energietechnik, TU-Berlin, Marchstr. 18, 10587 Berlin, Germany

(*Received* 10 *May* 1993 *and in final form* 31 *August* 1993)

Abstract—Three different types of quenching experiment have been conducted with a hollow copper cylinder of 50 mm length, 10 mm I.D. and 32 mm O.D. for pressure from 0.1 to 1.0 MPa, mass flux from 25 to 500 kg $m^{-2} s^{-1}$ and inlet subcooling from 5 to 50 K. The thermocouple delay in the installed condition has been carefully calibrated and a two-dimensional numerical method for solving inverse heat conduction problems was used in data reduction. The applicability of the experimental technique and parameter effects of the quenching process were discussed in detail. Quenching boiling curves were compared with the corresponding steady-state boiling curves obtained on the same test section and transient effects with respect to the global inlet conditions have been observed for a certain parameter range. The measured minimum film boiling temperature and critical heat flux were compared with physical models and correlations from the literature and a semi-empirical model for transition boiling heat transfer was proposed which shows satisfactory agreement with the present measurement results.

1. INTRODUCTION

DUE TO its importance for the metallurgical process and for evaluating the effectiveness of the emergency core cooling system of the water cooled nuclear reactors, quenching process is one of the most frequently discussed topics of the two-phase flow and heat transfer. Previously, quenching was the only simple way to measure the physically unstable transition boiling regime. After the invention of different types of temperature-controlled test sections, quenching experiments were thought to be inferior because of the inherent unsteady-state nature and difficulties related to the temperature measurement and the inverse solution of the heat conduction problem in the data reduction. As transition boiling usually occurs under transient conditions, a reverse question can be asked about the applicability of steady-state measurement results from temperature-controlled experiments for the real quenching process. Although a great deal of endeavor has been devoted since the pioneer work of Bergles and Thompson [1] to compare the steady-state and quenching boiling curves, a convincing and clear-cut conclusion has still not been achieved. This can be attributed to several nuisance factors, such as the change of surface condition and dynamic temperature measurement errors, which often accompany the quenching experiment and make it extremely difficult to separate their influences from possible transient effects. Compared with quenching processes under pool boiling conditions, those under well-controlled forced convective flow have been even less investigated [2–4].

In order to investigate the possible transient effect in the quenching process with careful consideration of the above-mentioned nuisance factors we have conducted both steady-state and quenching experiments on a single electrically heated temperature-controlled thick-walled test section with inside vertical flow.

In the present paper, emphasis will be given to the results of quenching experiments.

2. EXPERIMENTAL TECHNIQUE AND PROCEDURE

The water loop and test section used for the present quenching experiment are the same as those used by Weber *et al.* [5] for the steady-state temperature-controlled measurement of boiling curves.

The pressurized water loop (Fig. 1(a)) consists mainly of a centrifugal pump, filters, demineralizer, preheaters, three turbine flow meters with different measurement ranges, pressurizer, condenser and a cooler. The system pressure and inlet subcooling of the test section can be automatically maintained at the preset values within 1%. Mass flux through the test section can be adjusted manually through needle valves. Due-distilled water was used to fill the loop and a high purity was maintained with help of the demineralizer.

The test section (Fig. 1(b)) consists of a hollow cylinder of 50 mm length with an outer diameter of 32 mm and an inner bore of 10 mm. It is heated by ten cylindrical heating elements of 3 mm O.D., which are embedded coaxially on a circle of 11.5 mm. The hollow cylinder is made of oxygen-free, high conductivity copper of highest purity (Cu > 99.95%) and soldered under vacuum onto a monel tube of 0.15 mm wall thickness which serves as the flow channel.

To avoid the heat loss calibration of the test section

NOMENCLATURE

A_H	boiling surface area of a lumped-body [m^2]
C	equivalent time constant [s]
C_A	coefficient in equations (19)
c_p	specific heat capacity [J kg^{-1} K^{-1}]
D	inside diameter [m]
f	wetting fraction
G	mass flux [kg m^{-2} s^{-1}]
G^*	dimensionless mass flux
g	gravitational acceleration [m s^{-2}]
Δh_{fg}	evaporation enthalpy [J kg^{-1}]
h'', h'	specific enthalpy of vapor and liquid in saturation state [J kg^{-1}]
k	heat conductivity [W m^{-1} K^{-1}]
m	mass flux through vapor–liquid interface [kg m^{-2} s^{-1}]
P	system pressure [MPa]
p	local pressure of a single phase [MPa]
q	heat flux [W m^{-2}]
$q_{TB,E}$	experimental results of transition boiling heat flux [W m^{-2}]
$q_{TB,M}$	estimation of transition boiling heat flux [W m^{-2}]
q_g	heat flux from vapor phase to interface in interface coordinates [W m^{-2}]
q_w	heat flux from liquid phase to interface in interface coordinates [W m^{-2}]
q_g^*	heat flux from vapor phase to interface in transformed coordinates [W m^{-2}]
q_w^*	heat flux from liquid phase to interface in transformed coordinates [W m^{-2}]
T_{ref}	mean wall temperature [°C]
ΔT_{sub}	inlet subcooling [K]
T_g	saturation temperature of vapor [°C]
T_s	saturation temperature [°C]
T_w	wall temperature or saturation temperature of the wetting liquid [°C]
u	specific internal energy [J kg^{-1}]
V	volume [m^3]
v	specific volume [m^3 kg^{-1}]
v'', v'	specific volume of vapor and liquid at saturation condition [m^3 kg^{-1}]
w	velocity [m s^{-1}]
z	axial coordinate [m].

Greek symbols

ρ	density [kg m^{-3}]
μ	dynamic viscosity [kg m^{-1} s^{-1}]
σ	surface tension [N m^{-1}]
τ	time [s].

Subscripts

b	unstable nucleate boiling
CHF	critical heat flux condition
crit	thermodynamic critical state
f	unstable film boiling
g	vapor phase
Leid	Leidenfrost condition
l	bulk liquid
min	minimum film boiling condition
r	reduced thermodynamic state
s	saturation state
TB	transition boiling
w	liquid phase wetting the wall
σ	vapor liquid interface.

with complicated geometry, which seems practically unsolvable, especially under transient conditions, the test section is heavily instrumented with 32 sheathed NiCr–Ni micro-thermocouples in order that the transient temperature field can be determined from inside temperature measurements, only. There is one row of eight thermocouples of 0.25 mm O.D. passed through holes of 0.6 mm diameter from the outer cylinder surface and soldered onto the outer surface of the monel tube while simultaneously soldering the entire copper cylinder on it. The average distance of the thermocouple beads from the centerline is 5.39 mm which results from individual determination of each bead location using X-ray photographs. Three further rows of thermocouples of 0.5 mm O.D. are embedded within the copper cylinder at three different radial planes (mean radial locations of the beads from the centerline are 6.99, 8.89 and 9.79 mm, respectively) within thermocouple holes of 0.6 mm diameter, press-fitted and fixed by individual clamps. The press-fitting does not provide ideal thermal contact, its influence, however, can be properly considered, as will be discussed later. Heat supply to the test section is accomplished by a D.C. power amplifier (15 V, 2500 A) which can be controlled manually or automatically with a function generator.

The data acquisition and part of the data processing are accomplished by a personal computer together with a Keithley Series 500 Data Acquisition and Control System. The Soft-500 software package controls the data scanning, conversion of the data into engineering units and the storage of the results. The sampling frequency of 10 Hz has proved to be high enough to follow the transient, yet without causing unacceptable storage requirement.

Once the inlet conditions (pressure, mass flux and inlet subcooling) of the test section are stabilized to the preset values, quenching experiment can be started. With help of the temperature-controlled heating system, three different types of quenching experiment can be conducted.

Type A. The test section is heated using the tem-

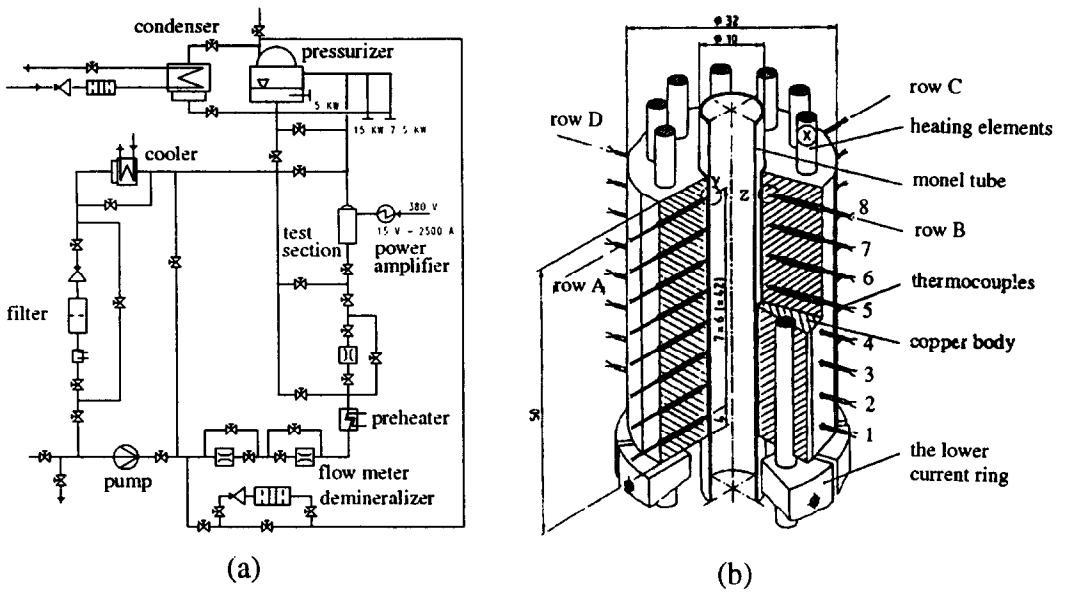

FIG. 1. Sketch of the pressurized water loop and the structure of the indirectly heated temperature-controlled test section.

perature-controlled system up to the stable film boiling regime, while keeping water flow through the test section. With the help of the internal and external modes (manual and automatic controls) of the power amplifier, the temperature-controlled heating can then be changed to heat flux controlled heating without disturbing the established film boiling. After 5 min of stabilization, the heat supply to the test section is gradually reduced using a function generator until rewetting of the heat transfer surface occurs.

Type B. The procedure of establishing the stable film boiling is the same as that for the type A experiment. However, quenching is initiated by suddenly shutting down the total power supply to the test section.

Type C. The water flow through the test section is at first diverted to a bypass. The test section is then heated up to about 420°C, while the heat transfer surface is protected with nitrogen gas. Water flow is then introduced into the test section. This is the traditional way of carrying out quenching experiments. This type of quenching experiment can only be conducted under atmospheric pressure with the present water loop.

3. THERMOCOUPLE CALIBRATION AND DATA REDUCTION

As mentioned above, the calibration of heat losses from the test section to the surrounding can be avoided by estimating temperature and heat flux on the boiling surface from the measured inside temperature histories only. This means that careful consideration of temperature measurement error is essential for the accuracy of the final experimental results, especially when the two-dimensional inverse heat conduction problem is to be solved, which may be extremely sensitive to temperature scatter. Generally, the temperature measurement error consists of two parts, i.e. steady-state error and dynamic error. The first one is concerned with the inexact description of the thermoelectrical characteristic of an individual thermocouple, which has been calibrated in the present study with respect to a standard PT-100 resistance thermometer. The second part of temperature measurement error is caused by the thermal capacity of the thermocouple head and by the imperfect contact between thermocouple head and the test section wall as well as the inhomogeneity of the test section wall due to the embedment of thermocouples. This type of temperature measurement error can only be calibrated on the already instrumented test section. To do so, the test section, thermally insulated on the outside surface and protected on the inside surface by nitrogen gas, is suddenly supplied with a constant electrical power. For this relatively simple boundary condition, an analytical solution of the temperature field inside the test section wall can be obtained, which quickly develops into a linear function of time after the application of the heating power. This has been confirmed by measurement results. The linear variation of the temperature field implies that the temperature difference between two specific positions is a constant. As the thermocouples of the first row are carefully soldered on the outside surface of the monel tube and have a smaller diameter than thermocouples of the remaining rows, it is reasonable to assume that they give exact measurement if the time constants of the thermocouples themselves are taken into consider-

ation. The real wall temperature on a specific position inside the test section wall can then be calculated from the temperature difference with respect to the first row. From the discrepancy between the estimated real temperature and the thermocouple reading the equivalent time constant of a thermocouple can be calculated.

A similar procedure to correct the dynamic temperature reading of embedded thermocouples has been used prior to this study by Auracher [6] for measuring boiling heat transfer of R-114. The transient temperature field was induced in this study by applying a sinus heating power on the test section.

The estimation of the temperature and heat flux distributions on the boiling surface from the corrected temperature histories inside the test section wall requires the solution of a two-dimensional inverse heat conduction problem, which is mathematically ill-posed and is very sensitive to the random temperature measurement error.

An efficient and stable numerical procedure relevant to the configuration and instrumentation of the present test section has been developed [7]. The method may be loosely interpreted as a mixture of solution of the differential heat conduction equation and pure interpolation of the temperature measurements. One example of the latter procedure can be found in ref. [8]. The definition of an overdetermined heat conduction problem in the method not only allows an efficient use of all measurement information but also helps to further account for the inhomogeneity of the heat conducting wall caused by embedment of thermocouples, which are not taken into account by the differential heat conduction equation. The extrapolation of the calculated temperature field to the boiling surface has been conducted by introducing a two-dimensional hyperbolic differential heat conduction equation. The inclusion of an additional second-order derivative of temperature with respect to time incorporates automatically the future temperature information, which is an efficient way of ensuring numerical stability. For a detailed description of the numerical procedure, reference may be made to ref. [7].

Due to the existence of a moving rewetting front, the time rate of change of wall temperature at different stages of the quenching process and at different axial locations varies considerably. An efficient data reduction method requires the use of varible time steps. This is achieved in the present case by representing the temperature measurement of each thermocouple with a third order spline function. In order to avoid unwanted distortion of the original information, the grid points of the spline function have been chosen to be extremely dense, with each sampling point representing a grid point. The weak filtration of noise by this kind of spline function is strengthened by inclusion of a digital filter.

A simplified error analysis of the present numerical method by using an analytical example to generate artificial measurement data shows that for the input thermocouple readings with a standard deviation of 2 K the error of estimated surface temperature is less than 4 K, and the error of the surface heat flux is less than 10% if the heat flux is higher than 1.5 MW m^{-2}, and is less than 30% for heat flux around 0.5 MW m^{-2}.

4. ASSESSMENT OF THE EXPERIMENTAL TECHNIQUE

4.1. *Influence of thermocouple delay on the calculated boiling curves*

Due to the obvious risk of destruction of the electrical insulation of the heating elements, only four calibration tests with different rates of change of wall temperature have been conducted. Now it can be investigated how the dynamic temperature measurement error may deteriorate the accuracy of the estimated temperature and heat flux on the boiling surface and whether the correction with the equivalent time constants described above is sufficient. Figure 2 shows three boiling curves that are calculated from a single quenching experimental run but with different equivalent time constants for the 24 thermocouples that are press-fitted. The first case uses the average value of the time constants from all four calibration tests, as is always so for results given in the following sections. In the second case, time constants from only one calibration test is taken into consideration. The difference between these two cases seems to be negligible, implying that four calibration tests are sufficient to correct the dynamic error. If, however, the imperfect contact between thermocouples and the test section wall is not corrected at all in the third case, i.e. only the time constant of the thermocouple itself is considered, large errors appear, especially around the CHF region, which amounts to as much as 20% for the surface heat flux, with the boiling curve in the nucleate boiling regime shifting towards lower wall superheat.

4.2. *Lumped-body, one-dimensional and two-dimensional data reduction methods*

Many of the early quenching experiments were evaluated with the lumped-body model, which defines that the average surface heat flux is proportional to the rate of change of wall temperature measured on a specific location. The very common one-dimensional data reduction method for the thin-walled test section with the assumption of a constant propagation velocity of the rewetting front can be considered as the thermal capacity being lumped in the radial direction. With the development of numerical procedures for the solution of inverse heat conduction problems, one-dimensional instrumentation and data reduction are more frequently employed in the quenching experiment with two or more thermocouples being distributed in the normal direction of the heat transfer surface. As the quenching process under convective

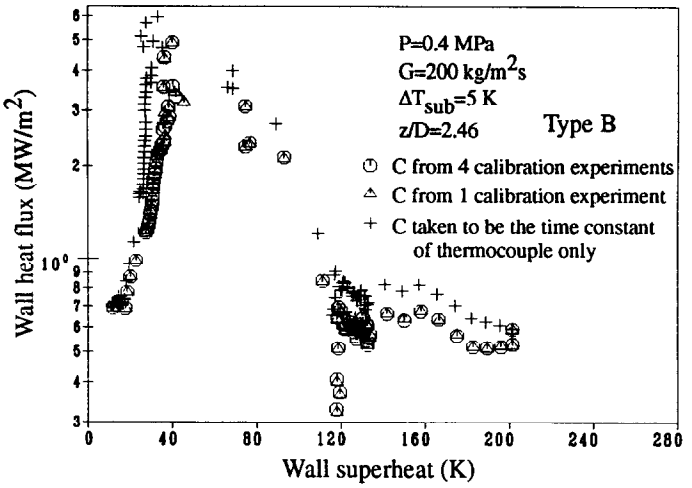

FIG. 2. Influence of dynamic error on the estimated boiling curve.

flow, possibly also under pool boiling conditions, is accompanied by one or more moving quenching fronts, a large temperature gradient also occurs along the heat transfer surface. This may result in a significant error in the estimated surface heat flux if a lumped-body or one-dimensional data reduction model is used. The present 2-d data reduction method can be artificially degenerated to a 1-d method when only four thermocouples on the same axial location, e.g. A4, B4, C4 and D4 are selected, whereas the temperature readings of the remaining thermocouples are identified with that of one of the selected thermocouples lying on the same row. However, the same degeneration procedure cannot be extended to the lumped-body model, since an infinite thermal conductivity is assumed in the latter, which is not the case in the present numerical procedure. Instead, the lumped-body model is directly established for the present copper test section,

$$-qA_H = \rho V c_p \frac{dT_w}{d\tau} \quad (1)$$

in which A_H is the total area of the boiling surface and T_w is the temperature reading of a specific thermocouple, e.g. A4. The temperature drop from the measurement location across the monel tube to the boiling surface is estimated simply by one-dimensional heat conduction. The estimated quenching boiling curves from a single experimental run using the above mentioned three methods are compared in Fig. 3. As was expected, the two- and one-dimensional data reduction methods do not give apparent differences for the nucleate boiling regime due to the insignificant axial temperature gradient. Large discrepancies, however, occur for the lower part of the transition boiling regime and intermediate film boiling regime. The one-dimensional data reduction cannot account for the large axial temperature gradient around the local Leidenfrost point. The good agreement between the two methods in the upper part of the transition boiling regime, where a large axial temperature gradient is also present, implies that the axial heat flux into a control volume is about equal to the axial heat flux leaving the control volume. This may happen to occur for a central location and has also been observed by Cheng *et al.* [2]. More interesting is the comparison of the lumped-body model with the one- and two-dimensional data reduction methods. The significant shift of the estimated boiling curve to the right-hand side shows how misleading the lumped-body model may be, if a moving rewetting front is present. The large scatter of quenching boiling curves from the literature can partially be attributed to the insufficient description of the dimensionality of the quenching phenomenon. The lumped-body model given by equation (1) is only valid for an ideal material with infinite heat conductivity. However, for quenching processes involving rewetting fronts on a test section made from material with limited thermal conductivity, the temperature drop is not only caused by the radial heat flux but also by the axial conduction which is not accounted for by the lumped-body model, so that it overestimates the radial heat flux. The turning point of the measured temperature trace, which corresponds to the critical boiling condition estimated by the lumped-body method, does not mean the real maximum radial heat flux, it is only the competing result of the increasing radial heat flux and the decreasing axial heat flux. After the turning point the lumped-body model underestimates the radial boiling heat flux.

4.3. *Repeatability of quenching boiling curves*

The stochastic nature of boiling phenomenon, especially in transition boiling regime, results in the fact that the local boiling curve can only be repeated in the sense of time average. For the steady-state measurement the data scatter may be considerably

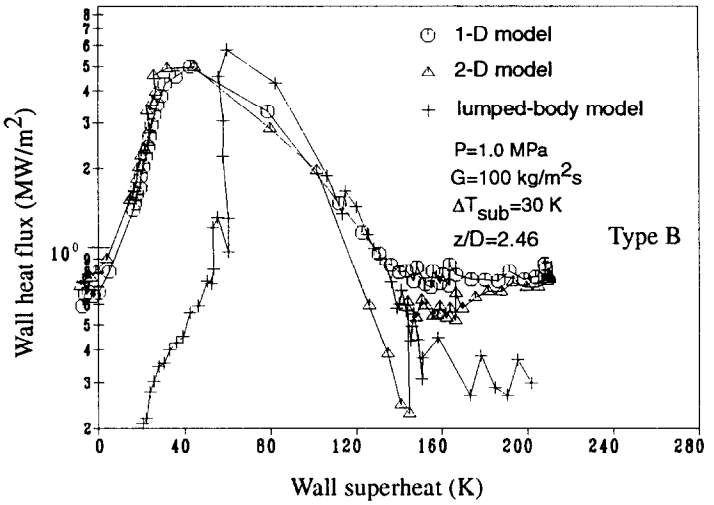

FIG. 3. Comparison of different data reduction methods.

reduced by averaging a large number of sampling points within a measurement duration. Obviously, the same procedure is not possible for the fast transient process. Instead, small scatter can only be achieved by smoothing the original data with spline functions or digital filters and by reducing the sensitivity of the data reduction method to the temperature measurement error. For a large time span, repeatability means the stability of the characteristics of the involved experimental facility. This may include the surface condition and thermal contact between thermocouples and the test section wall. Their consequencies have been minimized in the present case by intensively carrying out all the experiments within three months. With help of all these provisions a good repeatability of quenching boiling curves has been achieved as is shown in Fig. 4.

Good repeatability of the experimental results requires also that the data reduction method is not sensitive to the time steps which are chosen to some extent arbitrarily according to the rate of change of wall temperature at different stages of the quenching process. Figure 5 shows that the estimated boiling curves with three different sets of time steps agree well with one another.

5. EXPERIMENTAL RESULTS

A total number of 180 effective runs of quenching experiments of different types have been conducted with the following parameter matrix:

Pressure: 0.1, 0.4, 0.7, 1.0 MPa
Mass flux: 25, 50, 100, 200, 300, 500 kg m^{-2} s^{-1}
Inlet subcooling: 5, 15, 30, 50 K.

However, not all matrix points can be measured on

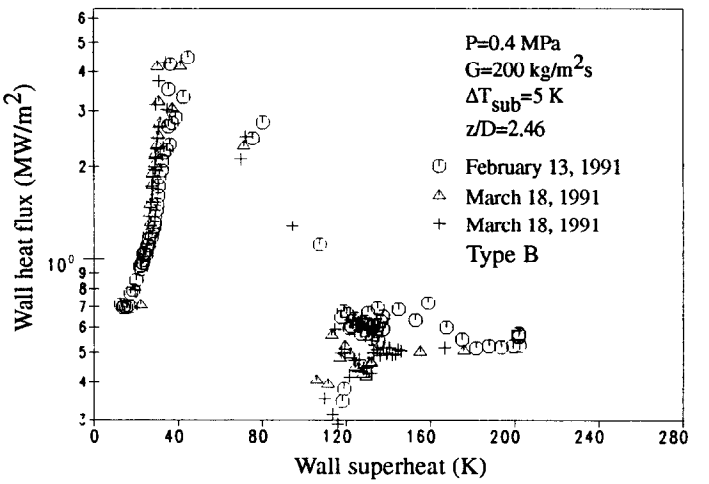

FIG. 4. Reproducibility of quenching boiling curves.

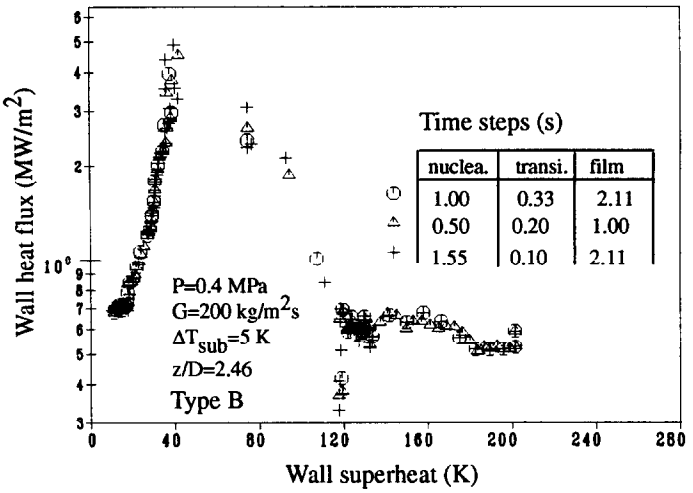

FIG. 5. Influence of time steps on the estimated boiling curve.

the present water loop. For low mass flux and small inlet subcooling, flow instability may occur due to vapor production on the preheaters. The upper limit of inlet subcooling is limited by mechanical vibration caused by violent vapor condensation immediately above the outlet of the test section. For high mass flux the limitation of the inlet subcooling is additionally imposed by the unacceptable high wall temperature that occurs on the outlet part of the test section during establishing the stable film boiling using the temperature-controlled heating system. It should be pointed out that most quenching experiments carried out in the present study are of type A and B because of the much lower scatter of the measured quenching boiling curves and the current inadequacy of the water loop for carrying out the third type of quenching experiment under pressurized conditions.

5.1. *Quenching starting from different boiling regimes*

Most quenching experiments carried out in the present study start from the stable film boiling regime. Rewetting of the heat transfer surface begins when the local temperature falls below the minimum film boiling temperature. As the temperature-controlled heating system allows the average surface temperature to be held at any given value at steady-state conditions, quenching from other boiling regimes can also be investigated.

For steady-state boiling under forced convective conditions, a large axial temperature gradient occurs, especially in the transition boiling regime, so that the temperature level of the heat transfer surface can only be represented from the average point of view. In the present study we use the average reading of three thermocouples of the first row (A2, A4 and A6) T_{ref}. Boiling curves on a midplane of the flow channel from quenching experiments for four different starting wall temperatures are compared in Fig. 6. For $T_{ref} = 384°C$ the whole heat transfer surface is located in the film boiling regime, while for $T_{ref} = 301°C$ all nucleate, transition and film boiling modes exist simultaneously one behind another along the flow direction. This can be easily recognized from the temperature traces at three measurement locations and their fluctuations incorporated in the upper part of the figure. The last two cases correspond to nucleate boiling mode on the whole boiling surface with $T_{ref} = 239$ and 219°C, respectively. The first of the two lies immediately before the critical heat flux condition. Boiling curves shown in Fig. 6 illustrate some quite unexpected good agreement, except for the shaded part of the data points for $T_{ref} = 301°C$. They represent the transition period from the steady-state initial condition to the transient quenching process. Their deviation from the main part of the data points is consistent with the global transient effect in the transition boiling regime to be discussed in a later section. It seems that for the present short test section, wall temperature is the predominant influencing parameter for the heat flux compared with the possible change of vapor distribution or flow form. Slight deviation can only be recognized in the nucleate boiling regime. Except for the quenching experiment with $T_{ref} = 219°C$, the boiling curves in the nucleate boiling regime displace slightly towards lower wall superheat with the increase of starting wall temperature. This may be due to the larger number of bubble sites that remain active for the higher starting wall temperature after the critical heat flux point has been traversed.

5.2. *The influence of axial position*

To avoid possible entrance and outlet effects only boiling curves on the midplane of $z/D = 2.46$ are used for the analysis of the quenching results. However, it is interesting to know how strongly the boiling curve

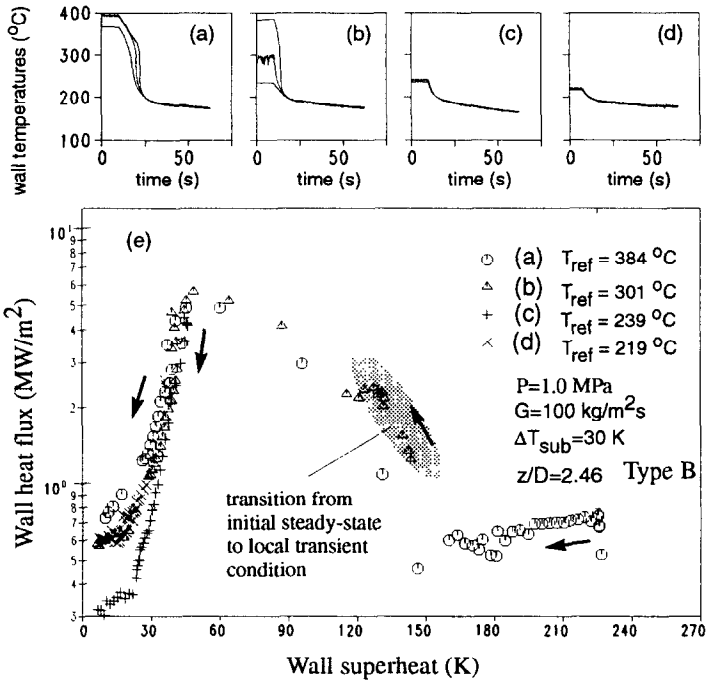

FIG. 6. Comparison of quenching processes from different boiling regimes.

is dependent on the axial position. In Fig. 7 boiling curves at three different axial positions are compared for two different starting wall temperatures of the quenching process. One of the quenching processes starts from the stable film boiling regime and the other from nucleate boiling regimes. For both cases the boiling curves at different axial positions agree reasonably well with each other, although there is apparent data scatter in the transition boiling regime, which, however, does not reveal any systematic trend. A slight decrease of wall heat flux with the increase of axial distance from the inlet can be recognized in the film boiling regime. This is obviously due to the poor heat conducting vapor film, which becomes thicker in the flow direction.

The insensitivity of the local boiling curve with respect to the axial position is attributed on the one hand to the relative short test section, which does not facilitate significant change of local vapor quality and on the other hand to the lower propagation velocity of rewetting front with respect to the liquid velocity. The propagation velocity of the rewetting front, which

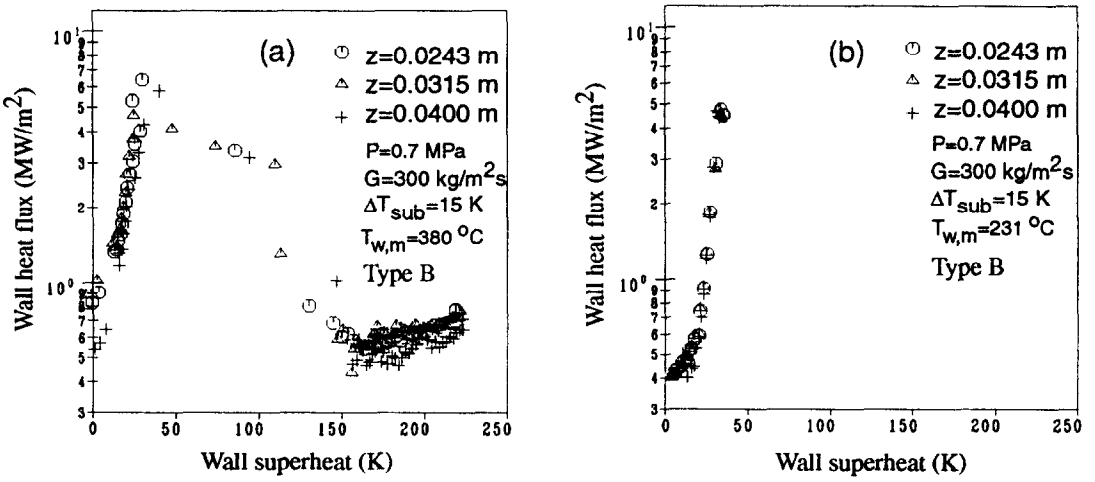

FIG. 7. The influence of axial position on local boiling curves.

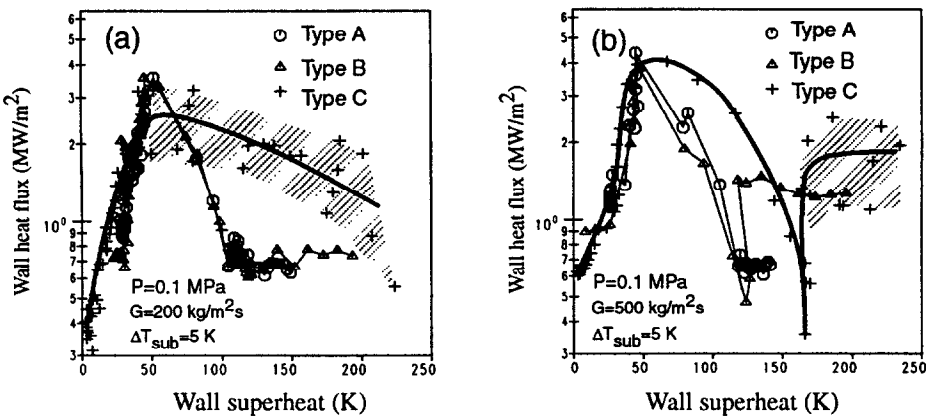

FIG. 8. Comparison of boiling curves from three different types of quenching experiment at atmospheric pressure.

is estimated to be about 0.01 m s^{-1}, is apparently smaller than the average liquid velocity between 0.05 and 0.5 m s^{-1}. In this case the axial distribution of vapor quality ahead of and behind the moving rewetting front may not change significantly with time. For even lower mass flux of upward flow, the situation may not change since the rising velocity of bubbles within a still liquid pool is about 0.20 m s^{-1}, which is still higher than the propagation velocity of the rewetting front. An apparent axial dependence of boiling curve on axial position may be expected for downward flow. In this case the distribution of void fraction behind and ahead of the rewetting front may change due to the counter current flow of vapor and liquid.

5.3. *Influence of inlet conditions*

The parameter influence of the inlet conditions, i.e. the pressure, inlet subcooling and mass flux was described in detail in a previous report [9]. In summary, the system pressure is the predominant influencing parameter, which improves heat transfer in all boiling regimes except film boiling. The increase of mass flux improves heat transfer in post critical boiling regimes, obviously due to the more efficient vapor transport ability and the increased flow turbulence. The influence of the inlet subcooling is insignificant for all boiling regimes.

5.4. *Comparison of different types of quenching experiment*

As mentioned above, quenching from the established steady-state film boiling can be initiated either by gradually reducing (Type A) or suddenly cutting off (Type B) the power supply to the test section. As is shown in Fig. 8, the difference of the measured boiling curves from these two types of quenching experiments is not significant. Because the heat flux before the start of rewetting of the heat transfer surface is only about one tenth of its critical value, the transient heat conduction within the test section wall does not seem to be considerably influenced by the still remaining heat supply during a quenching experiment of Type A. However, if we compare these two types with Type C quenching experiment, where water is suddenly diverted into the heated dry test section, significant difference can be observed both for low and high mass flux. For low mass flux, large wall temperature fluctuation was observed also when the surface temperature is well above the Leidenfrost temperature. No inverted annular flow seems to exist. There seems to be considerable sputtering on the flow front and consequently strong liquid entrainment which also improves the heat transfer in the downstream region. As a result, the estimated boiling curves have large scatter with the average heat transfer rate in the transition boiling regime being much higher than that from the other two types of experiments. For mass flux higher than 300 kg m^{-2} s^{-1} the scatter of the boiling curve in the transition boiling regime is much smaller. There is obviously a rewetting front behind the moving flow front in this case. Cabajo [10] attributed this to the hydrostatic pressure exerted by the liquid column that stands above the rewetting front. The boiling curve from Type C quenching experiment for higher mass flux also shows a better heat transfer in transition boiling regime, as is illustrated in Fig. 8(b).

5.5. *Comparison of quenching boiling curves with steady-state boiling curves*

One of the important aspects of the present study is to compare quenching boiling curves with the steady-state boiling curves with the aim of identifying possible transient effects. Most of the steady-state measurements have been carried out on the same test section using temperature-controlled heating by Weber *et al.* [5, 8,11], but reevaluated with the present data reduction method to eliminate the influence of systematic error on comparing steady-state with transient results. During the temperature-controlled

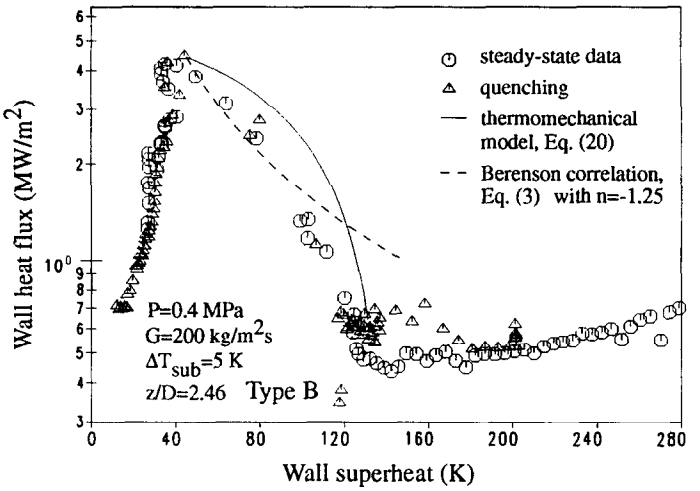

FIG. 9. Comparison of quenching boiling curve with steady-state boiling curve for low parameter range.

measurements, the average surface temperature can be held at any preselected value or changed in a quasi-steady-state manner. The present quenching process, which finishes within about one minute after rewetting establishes, is very fast compared with the quasi-steady-state measurement, which usually takes one hour to traverse a single boiling curve. As examples, boiling curves from both types of experiments are compared in Figs. 9 and 10 for two different inlet conditions. A systematic comparison of all experimental results shows that for the parameter range of $P < 0.7$ MPa, $G < 300$ kg m^{-2} s^{-1} and $\Delta T_{sub} < 15$ K there is no significant difference between the quenching and steady-state boiling curves in all boiling regimes. Beyond this range, however, the difference becomes obvious in the transition boiling regime. Quenching boiling curves lie below the corresponding steady-state boiling curves. The minimum film boiling temperature from quenching is apparently lower than that from the steady-state measurement, implying that the vapor film is more stable in the former case. After the sudden collapse of the vapor film, it seems that vapor bubbles formed on the heat transfer surface cannot be moved away efficiently, resulting in a smaller heat flux compared with the steady-state measurement for the same inlet conditions. However, the situation improves with the further decrease of the wall superheat. At CHF points the transient effects almost disappear except at very high mass flux, i.e. $G > 500$ kg m^{-2} s^{-1}, for which the transient critical heat flux from quenching is somewhat lower than the steady-state value.

The above observed difference between the steady-state and quenching boiling curves can be termed transient effects with respect to the global inlet conditions. Strictly speaking, transient effects should be

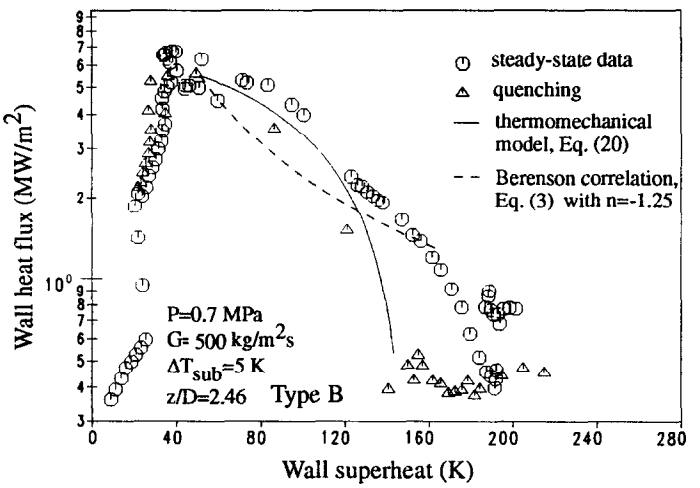

FIG. 10. Comparison of quenching boiling curve with steady-state boiling curve for high parameter range.

defined as the difference of local heat transfer between transient and steady-state processes for the same surface conditions and the same local thermohydraulic conditions: pressure, mass flux and vapor quality (possibly vapor void fraction). A literature survey shows that this kind of experiment has not been conducted so far. This is obviously due to difficulties associated with exactly measuring or estimating the local flow parameter under highly transient conditions.

It has still proved to be a very challenging task to identify possible transient effects with respect to global inlet conditions, because other parameters such as surface conditions and accuracy of temperature measurement can hardly be kept the same for both cases. Bergles and Thompson [1] have conducted the first systematic comparison of steady-state and quenching heat transfer under pool boiling conditions for water, Freon-113 and liquid nitrogen. Apparent differences have been observed for all the three cases, which, however, could not be simply attributed to the transient effects of the quenching process. Besides the different test piece materials used for steady-state and quenching experiments, the surface condition has considerably changed during the quenching experiment due to heating up of the test pieces with an oxy-acetylene torch flame (for water and Freon-113) and due to frost forming (for liquid nitrogen). The existence of the rewetting front along the heat transfer surface under pool boiling conditions has additionally contributed to the uncertainty both in temperature measurement and in data reduction.

In the present study the influence of these nuisance factors has been eliminated or minimized by using the same test section and the same data reduction method for both steady-state and quenching experiments and by carefully calibrating the dynamic temperature measurement error. Therefore, the observed differences between the two kinds of experiments in Figs. 9 and 10 are only related to the transient nature of the quenching process and the characteristics of the temperature-controlled steady-state measurement. Transient effects with respect to local conditions may contribute to the observed discrepancy, but the conjugate effect of heat conduction within the test section wall and the convective boiling heat transfer on the local thermodynamic conditions is believed to be the major factor. For the steady-state measurement the transition boiling usually occurs not alone, but simultaneously with nucleate boiling or film boiling or both on the boiling surface. This results in large axial temperature gradient and high wall temperature at the outlet of the test section. For $P = 0.7$ MPa, $G = 500\ \mathrm{kg\ m^{-2}\ s^{-1}}$ and $\Delta T_{sub} = 15$ K, an axial temperature difference of as much as 200 K with the wall temperature at the outlet of as high as 420°C has been measured on the present thick-walled copper test section. Similar temperature level and heat flux distribution will not occur during quenching experiments. When rewetting first begins from the inlet of the test section, the surface temperature at all axial positions are below 340°C and the wall temperature will never rise again during the course of rewetting. Another special problem related to the steady-state measurement with an electrically heated test section is that the stability criterion for the temperature control cannot always be satisfied in the sense of second order if the surface reference temperature is not properly chosen [12]. As a consequence, some parts of the local boiling curve can never be accessed. A similar problem does not exist for quenching boiling curves.

6. ANALYSIS OF THE QUENCHING RESULTS

Due to the requirement of complicated experimental technique and its inherent unstable nature, transition boiling remains the least understood boiling regime. Therefore, we will concentrate our following data analysis on this boiling regime, although a complete boiling curve can be obtained from a single quenching experiment.

Generally, the description of the heat transfer in the transition boiling regime has been based on the work of Berenson [13], who concluded from the experimental observations that transition boiling can be treated as the unstable nucleate boiling and unstable film boiling alternately existing on the same location. The decrease of the heat flux with increasing wall temperature can then be attributed to the changing time portion, during which each boiling mode exists. This can be formulated as

$$q_{TB} = fq_b + (1-f)q_f \tag{2}$$

where q_b and q_f designate the heat fluxes due to unstable nucleate and film boiling, respectively, while f is the wetting fraction. Although equation (2) is conceptually quite simple, its application has encountered great difficulty because both q_b and q_f are hypothetical themselves and unknown. A common practice is to assume that $q_b = q_{CHF}$ and $q_f = q_{MIN}$ and that the wetting fraction can be described as a simple function of wall temperature, so that the critical heat flux condition and the minimum film boiling point (Leidenfrost point) act as two anchor points. Depending on the way of chosing the anchor points, different types of correlations have been developed in the literature. In the often cited Berenson correlation, it was assumed that

$$f = \left(\frac{T_w - T_s}{T_{CHF} - T_s}\right)^n \tag{3}$$

with $q_b = q_{CHF}$, $q_f = 0$.

It is clear that the two limit conditions, i.e. the CHF and the Leidenfrost points, play an important role in describing the heat transfer in the transition boiling regime. We will therefore first compare our present measurement results of these two characteristic conditions with correlations and physical models in the literature. The thermomechanical model for the Leid-

enfrost phenomenon at low vapor quality [14] will then be extended for the transition boiling regime.

6.1. *Critical Heat Flux condition*

Except for pool boiling there are few analytical models for the critical heat flux condition. Most engineering applications are based on the large number of correlations developed in the literature for different parameter ranges and geometries. Weber [11] has compared 11 correlations with 194 CHF data for low flow and low pressure conditions and arrived at the conclusion that the correlation proposed by Katto and Ohno [15] has the widest range of applicability. Using the same dimensionless groups, Weber developed a new correlation based on the collected CHF data and his own measurement results on a temperature controlled short test section. However, comparison of both correlations with the present results from quenching experiments has shown large scatter, obviously due to the small L/D of the present test section and the transient nature of the quenching process.

For this reason a new correlation has been developed using similar dimensionless groups:

$$\frac{q_{\mathrm{CHF}}}{G\Delta h_{\mathrm{fg}}} = 0.1754\left[\frac{\rho_{\mathrm{g}}}{\rho_{\mathrm{l}}}\right]^{0.001} G^{*-0.8} \tag{4}$$

with the dimensionless mass flux defined as

$$G^{*} = \frac{G}{\rho_{\mathrm{g}}^{1/2}[(\rho_{\mathrm{l}}-\rho_{\mathrm{g}})\, g\sigma]^{1/4}}. \tag{5}$$

This correlation can reproduce the present measurement data with satisfactory accuracy (6.3% mean deviation; 7.8% mean square error). Equations (4) and (5) and the Katto–Ohno correlation are compared with the present data in Fig. 11. The new correlation is based on much less data than that by Katto and Ohno, but it can serve as a more accurate representation of the anchor point for our own transition boiling data obtained from the transient quenching process.

6.2. *Minimum film boiling temperature*

A lot of terms have been used in the literature to define the boundary between film and transition boiling regimes, such as the minimum film boiling temperature, Leidenfrost temperature, true quench temperature, maximum transition boiling temperature, sputtering temperature and apparent quenching temperature. Except for the first three definitions, all the others may depend sensitively on the experimental configurations. For our present investigations, where the inverted annular flow generally occurs at the minimum heat flux conditions, we identify the minimum film boiling temperature with the Leidenfrost temperature.

The first thermodynamic model for the minimum film boiling temperature was proposed by Spiegler *et al.* [16]. The authors identified the minimum film boiling temperature with that corresponding to the maximum superheat of the metastable liquid proposed by Meyer [17] which can be derived from the Van der Waals equation of state:

$$T_{\mathrm{r}} = \frac{9}{4}\frac{(v_{\mathrm{r}}-1/3)^{2}}{v_{\mathrm{r}}^{3}} \tag{6}$$

and

$$P_{\mathrm{r}} = \frac{3}{v_{\mathrm{r}}^{2}} - \frac{2}{v_{\mathrm{r}}^{3}} \tag{7}$$

with $P_{\mathrm{r}} = P/P_{\mathrm{crit}}$, $T_{\mathrm{r}} = T/T_{\mathrm{crit}}$, $v_{\mathrm{r}} = v/v_{\mathrm{crit}}$.

They represent an implicit functional relationship between the limit superheat of the metastable liquid and pressure, which reduces to

$$T_{\mathrm{r}} = \frac{27}{32} \tag{8}$$

for pressures approaching zero.

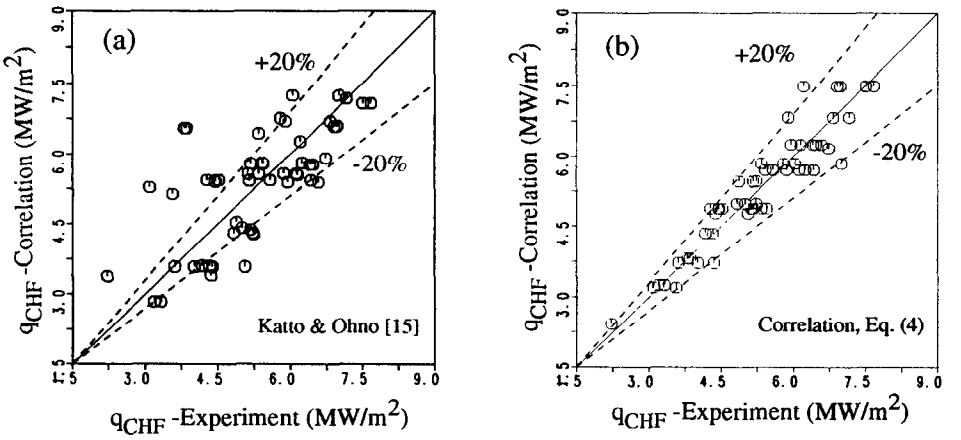

FIG. 11. Comparison of measured critical heat flux with correlations.

The calculated metastable limit of liquid according to Meyer model increases slightly with pressure. For water at high pressures, the predicted values are too low, even below the saturation temperature, indicating the invalidity of the Van der Waals equation of state close to the thermodynamic critical point. Nevertheless, Skripov [18] has shown that the Meyer model gives reasonable estimation of the maximum metastable superheat of water at moderate pressure compared with the experimental results of steam explosion. For the vanishing pressure, the Meyer model predicts a metastable limit of about 273°C using equation (8). The present experimental result of the Leidenfrost temperature of about 220°C at atmospheric pressure and the result of Testa and Nicotra [19] of 100°C for subatmospheric pressures down to 0.0033 MPa obviously do not support the assumption of Spiegler *et al.* that the Leidenfrost temperature is the limit temperature of the metastable state of liquid.

The first hydrodynamic model for the minimum film boiling temperature was given by Berenson [20]. He started from the analytical model of Zuber [21] for the minimum film boiling heat flux of pool boiling and describes the heat transfer through the vapor film as a pure heat conduction problem. The vapor film thickness was also calculated according to the hydrodynamic stability condition but incorporating to some extent empirical interpolation. He finally arrived at the relation:

$$\Delta T_{\min} = 0.127 \frac{\rho_g \Delta h_{fg}}{k_g} \left[\frac{g(\rho_l-\rho_g)}{\rho_l+\rho_g}\right]^{2/3} \times \left[\frac{\sigma}{g(\rho_l-\rho_g)}\right]^{1/2} \left[\frac{\mu_g}{g(\rho_l-\rho_g)}\right]^{1/3}. \quad (9)$$

Equation (9) predicts too low values for pressures lower than 0.2 MPa, but too high values for higher pressures.

The extremely large discrepancy of the above two models from the present excrimental results and between themselves shows that they cannot satisfactorily explain the physical mechanism that occurs at the Leidenfrost point. This has already been identified by comparing the two models (among others) with the experimental results from literature for water [8] and other fluids from cryogens up to liquid metals [22]. It has been observed [17] but frequently ignored, e.g. [16], that the metastable state of superheated liquids cannot survive the disturbances of temperature and pressure which always accompany the boiling process, especially in transition boiling regime. Based on this consideration it has been assumed that the wetting liquid on the heat transfer surface is not at metastable but saturated state at elevated pressure:

$$T_w = T_s(p_w), \quad (10)$$

with $p_w > P$, whereas vapor is assumed to be saturated at the system pressure of the bulk liquid:

$$T_g = T_s(p_g), \quad (11)$$

with $p_g = P$. As the Leidenfrost temperature is always higher than the corresponding saturation temperature at the system pressure, there exists a substantial overpressure on the interface between vapor and liquid [14]. The mechanical non-equilibria resulting from the thermal boundary layer are the well-known cross fluxes in the non-equilibrium thermodynamics. It is usually addressed as the thermomechanical effects. In boiling processes the mechanical non-equilibrium results from the momentum change at the interface when vapor is ejected at a much lower density than that of the consumed liquid.

The analysis for the Leidenfrost temperature starts from the conservation equations at the interface (σ) between wetting zones (w) and dry patches (g) during transition boiling:

$$\rho_w(w_w-w_\sigma) = \rho_g(w_g-w_\sigma) = m, \quad (12)$$

$$p_w+\rho_w(w_w-w_\sigma)w_w = p_g+\rho_g(w_g-w_\sigma)w_g, \quad (13)$$

$$\left(u_w+\frac{w_w^2}{2}\right)\rho_w(w_w-w_\sigma)+p_w w_w+q_w = \left(u_g+\frac{w_g^2}{2}\right)\rho_g(w_g-w_\sigma)+p_g w_g+q_g, \quad (14)$$

where ρ, w and u designate the density, the velocity (normal to the interface) and the specific internal energy. The kinetic energy $w^2/2$ is not an objective parameter, but depends on the moving observer. Since equation (14) is valid for coordinates fixed at the interface, it is more convenient to transform the equations to a coordinate system fixed on the heat transfer wall. The corresponding heat fluxes on the vapor and liquid sides then become:

$$q_g^* = q_g+mw_g(w_g-w_\sigma), \quad (15)$$

$$q_w^* = q_w+mw_w(w_g-w_\sigma). \quad (16)$$

Reorganizing equations (12)–(16) leads to the enthalpy of evaporation

$$h''(T_g)-h'(T_w) = \tfrac{1}{2}[v''(T_g)-v'(T_w)] \times [p_s(T_w)-p_s(T_g)]+\frac{q_w^*-q_g^*}{m}, \quad (17)$$

when taking into account the different temperatures of vapor and liquid, equations (10) and (11). Equation (17) can be interpreted as the fact that the enthalpy of evaporation is provided by both heat conduction and by the mechanical energy released during the depressurization process of evaporation. Note that q_g^* must be zero in order to keep the vapor at the assumed saturation temperature. By neglecting q_w^*, a closed equation can be arrived at for the Leidenfrost temperature:

$$h''(T_g)-h'(T_{Leid}) = \tfrac{1}{2}[v''(T_g)-v'(T_{Leid})][p_s(T_{Leid})-p_s(T_g)]. \quad (18)$$

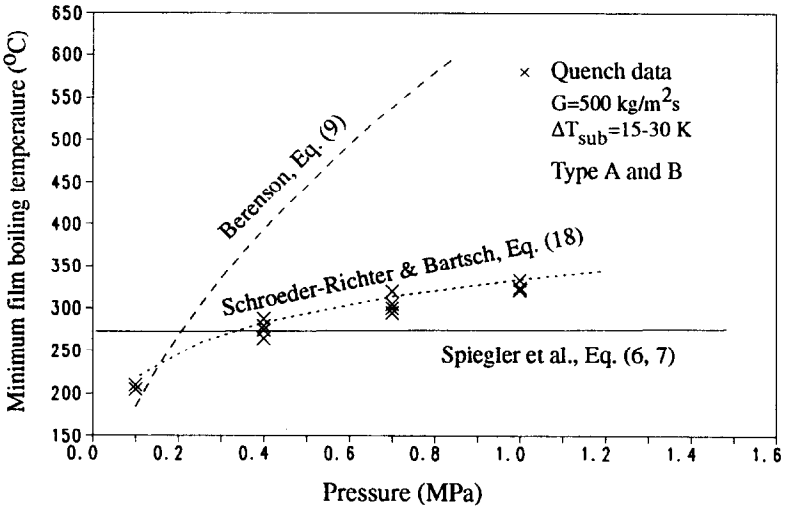

FIG. 12. Comparison of measured minimum film boiling temperatures with physical models.

The equation means that the enthalpy of evaporation at Leidenfrost point is supplied by the mechanical energy of depressurization alone.

A direct experimental verification of the assumed saturation condition on the boiling surface has not been tried yet, but comparison of equation (18) with experimental results from the literature for a variety of liquids from cryogenic coolants to liquid metals showed an astonishing wide range of applicability [14]. This is further supported by the present experimental results shown in Fig. 12. The slight scatter of experimental results for a fixed pressure displays the further dependences of the minimum film boiling temperature on mass flux and inlet subcooling (or local vapor quality). But pressure is obviously the predominant influencing parameter. The slight deviation of the data with respect to the prediction of equation (18) may also be partially attributed to the fact that the assumption of inverted annular flow form for the transformation of equations (15) and (16) may not be always satisfied.

6.3. *Transition boiling*

The thermomechanical model equation (18) for predicting the Leidenfrost temperature for low vapor quality will now be extended to build a semiempirical model for the transition boiling heat transfer. Besides the assumption of saturation condition for both liquid and vapor on the boiling surface, and thus equation (17), it is further assumed that the total heat flux on the boiling surface in transition boiling regime is proportional to the heat flux at the interface of liquid and vapor needed for evaporation:

$$q_{TB}(T_w) = C_A q_w^* = mC_A\{h''(T_g) - h'(T_w) - \tfrac{1}{2}[v''(T_g) - v'(T_w)][p_s(T_w) - p_s(T_g)]\}. \quad (19)$$

Fitting the unknown coefficient C_A to the anchor point at CHF leads to:

$$\frac{q_{TB}}{q_{CHF}} = \frac{h''(T_g) - h'(T_w) - \tfrac{1}{2}[v''(T_g) - v'(T_w)][p_s(T_w) - p_s(T_g)]}{h''(T_g) - h'(T_{CHF}) - \tfrac{1}{2}[v''(T_g) - v'(T_{CHF})][p_s(T_{CHF}) - p_s(T_g)]}. \quad (20)$$

The model distinguishes itself by the fact that no power formulation and fitting with transition boiling data (except CHF data) are necessary. For zero heat flux the model reduces to equation (18) for the Leidenfrost temperature, so that it does not have the weakness of most correlations and models in the high temperature transition boiling region. Equation (20) was compared with the present measurement data in Figs. 9 and 10 in the form of the boiling curve for the two specific inlet conditions. The advantage of the model concerning the curvature (convex form) of the boiling curve and the Leidenfrost point can be clearly seen. Both the present model and Berenson correlation are further compared with 200 data points in transition boiling regime in Fig. 13. To suppress the influence of the absolute value of the critical heat flux on the data point distribution, the comparison is conducted in the reduced form. It can be seen that the present model represents a considerable improvement compared with the Berenson correlation. A systematic convex shape can be clearly inferred from Fig. 13(a), while the data points distribute more uniformly along the diagonal in Fig. 13(b). Since equation (20) was derived from conservation equations, it may also be applicable to other fluids. This has been supported by the comparison of the model with the quenching data of Merte

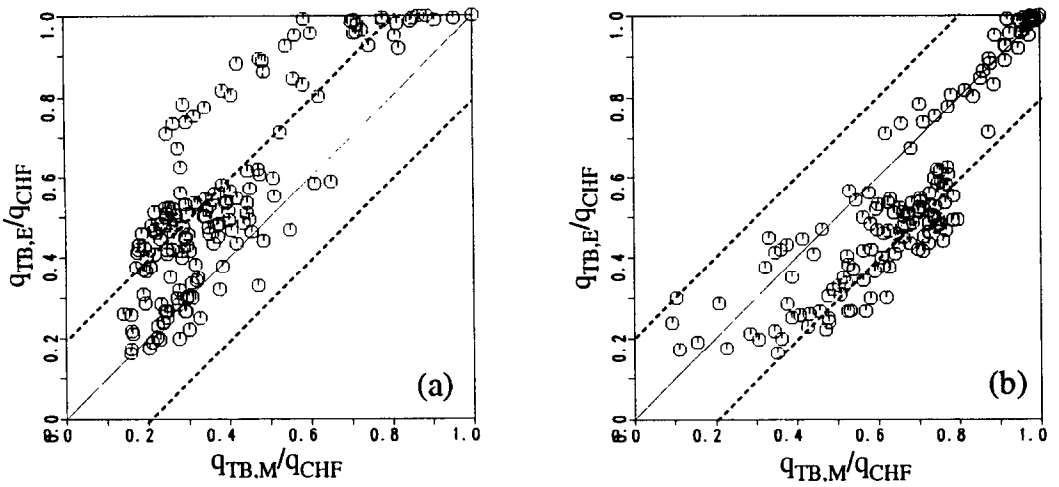

FIG. 13. Comparison of present transition boiling data with (a) Berenson correlation, equation (3), with $n = -1.25$ and (b) thermomechanical model, equation (20).

and Clark [23] for nitrogen in Fig. 14. The applicability of the model for other fluids is surely worth being further proved.

7. CONCLUSIONS

Parallel to the temperature-controlled steady-state measurements, quenching experiments under forced convective conditions have been conducted in three different ways on the same cylindrical test section for the inlet conditions of pressure from 0.1 to 1.0 MPa, mass flux from 25 to 500 kg m^{-2} s^{-1} and inlet subcooling from 5 to 50 K. It was found that careful calibration of the thermocouple delay in the installed condition and two-dimensional data reduction taking into account the axial temperature gradient are essential for the accuracy of the estimated quenching boiling curve. Using the same test section and the temperature-controlled heating for establishing stable film boiling has considerably improved the comparability of surface condition for steady-state and quenching experiments.

There exists a general trend that quenching boiling curve is traversed under smaller local vapor quality than the steady-state boiling curve for the same inlet conditions. This leads to the fact that some parameter dependencies, such as the axial location and inlet subcooling becomes less significant if compared with pressure and mass flux. This is also valid for different starting conditions of the quenching process (film, transition or nucleate boiling). This means that for the very short test section the local thermohydraulic condition relative to the moving rewetting front does not change significantly during the quenching process.

Transient effects with respect to global inlet conditions are not obvious for inlet conditions of $G < 300$ kg m^{-2} s^{-1}, $P < 0.7$ MPa and $T_{sub} < 15$ K. Beyond this range, the quenching boiling curves lie below the steady-state boilng curve in transition boiling regime, with the minimum film boiling temperature being correspondingly lower.

There is also an obvious difference between quenching of a heated dry tubc and quenching resulting from the collapse of the stable inverted annular flow.

The measured minimum film boiling temperature and critical heat flux were compared with physical models and correlations from the literature. A semi-empirical model for transition boiling heat transfer has been developed which includes the critical heat flux condition as the anchor point but does not use the power formulation. The model can predict the experimental results with reasonable accuracy.

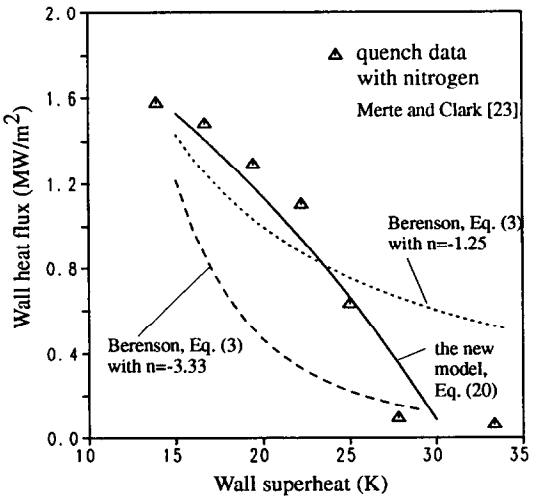

FIG. 14. Comparison of the thermomechanical model with nitrogen data from the literature.

REFERENCES

1 A. E. Bergles and W. G. Thompson, Jr., The relationship

of quench data to steady-state pool boiling data, *Int. J. Heat Mass Transfer* **13,** 55–68 (1970).
2. S. C. Cheng, W. W. L. Ng and K. T. Heng, Measurements of boiling curves of subcooled water under forced convective conditions, *Int. J. Heat Mass Transfer* **21,** 1385–1392 (1978).
3. W. J. Chen, Y. Lee and D. C. Groeneveld, Measurement of boiling curves during rewetting of a hot circular duct, *Int. J. Heat Mass Transfer* **22,** 973–976 (1979).
4. S. C. Yao and A. Salehpour, An investigation of transient boiling heat transfer with conjugate nature, *Int. J. Heat Mass Transfer* **26,** 901–909 (1983).
5. P. Weber, Q. Feng and K. Johannsen, Towards accurate measurement of post-CHF flow boiling heat transfer of water in a circular tube. In *Thermal-Hydraulic Fundamentals and Design, NATO ASI Series, Series E: Applied Sciences* (Edited by S. Kakac, A. E. Bergles and E. O. Fernandes), Vol. 143, pp. 210–219. Kluwer, Norwell, MA (1988).
6. H. Auracher, Transition boiling, *Heat Transfer 1990: Proc. 9th Int. Heat Transfer Conf., Jerusalem*, Vol. 1, pp. 69–96. Hemisphere, New York (1990).
7. X. C. Huang, G. Bartsch and B. X. Wang, A numerical method for solving the two-dimensional nonlinear inverse heat conduction problem with application to the study of transient boiling curves. In *Advanced Computational Methods in Heat Transfer, Vol I: Conduction, Radiation and Phase Change* (Edited by L. C. Wrobel, C. A. Brebbia and A. J. Nowak), pp. 381–397. Computational Mechanics Publications, Elsevier, Amsterdam (1992).
8. Q. Feng and K. Johannsen, Experimental results of maximum transition boiling temperature during upflow in a circular tube at medium pressure, *Exper. Thermal Fluid Sci.* **4,** 90–97 (1990).
9. X. C. Huang, G. Bartsch and B. X. Wang, Measurement of transient boiling curves of water during rewetting of a vertical circular tube. In *Transport Phenomena Science and Technology 1992* (Edited by B. X. Wang), pp. 397–402. Higher Education Press, Beijing (1992).
10. J. J. Carbajo, A study on the rewetting temperature, *Nucl. Engng Des.* **84,** 21–52 (1985).
11. P. Weber, *Experimentelle Untersuchungen zur Siedekrise und zum Übergangssieden von strömendem Wasser unter erhöhtem Druck*, No. 226. VDI Fortschritt-Bericht R3, Düsseldorf (1990).
12. X. C. Huang and G. Bartsch, About the second-order instability on the electrically-heated temperature-controlled test section under forced convective boiling conditions, *Int. J. Heat Mass Transfer* **36,** 2601–2612 (1993).
13. P. J. Berenson, Experiments on pool-boiling heat transfer, *Int. J. Heat Mass Transfer* **5,** 985–999 (1962).
14. D. Schroeder-Richter and G. Bartsch, The Leidenfrost phenomenon caused by a thermo–mechanical effect of transition boiling: a revisited problem of non-equilibrium thermodynamics. In *Fundamentals of Phase Change: Boiling and Condensation* (Edited by L. C. Witte and C. T. Avedisian) ASME-HTD-Vol. 136, pp. 13–20. ASME, New York (1990).
15. Y. Katto and H. Ohno, An improved version of the generalized correlation of critical heat flux for the forced convective boiling in uniformly heated vertical tubes, *Int. J. Heat Mass Transfer* **27,** 1641–1648 (1984).
16. P. Spiegler, J. Hopenfeld, M. C. F. Silberberg, C. F. Bumpus, Jr. and A. Norman, Onset of stable film boiling and the foam limit, *Int. J. Heat Mass Transfer* **6,** 987–989 (1963).
17. J. Meyer, Zur Kenntnis des negativen Drucks in Flüssigkeit, *Z. Elektrochemie* **17,** 743–745 (1911).
18. V. P. Skripov, *Metastabil'naia zhidkost: Metastable Liquids* (Translated by D. Slutzkin). Wiley, New York (1974).
19. P. Testa and L. Nicotra, Influence of pressure on the Leidenfrost temperature and on extracted heat fluxes in the transient mode and low pressure, *J. Heat Transfer* **83,** 916–921 (1986).
20. P. J. Berenson, Film-boiling heat transfer from a horizontal surface, *J. Heat Transfer* **83,** 351–358 (1961).
21. N. Zuber, On the stability of boiling heat transfer, *J. Heat Transfer* **80,** 711–720 (1958).
22. D. Schroeder-Richter, *Ein analytischer Beitrag zur Anwendung der Thermodynamik irreversibler Prozesse auf Siedephänomene*, No. 251. VDI Fortschritt-Bericht R3, Düsseldorf (1991).
23. H. Merte, Jr. and J. A. Clark, Boiling heat transfer with cryogenic fluids at standard, fractional and near-zero gravity, *J. Heat Transfer* **86,** 351–359 (1964).